

A New Approach to GraphMaps, a System Browsing Large Graphs as Interactive Maps

Debajyoti Mondal¹ and Lev Nachmanson²

¹Department of Computer Science, University of Saskatchewan, Saskatoon, SK, Canada

²Microsoft Research, Redmond, WA, U.S.A.

dmondal@cs.usask.ca, levnach@microsoft.com

Keywords: Network Visualization, Layered Drawing, Geometric Spanners, Competition Mesh, Network Flow

Abstract: A GraphMaps is a system that visualizes a graph using zoom levels, which is similar to a geographic map visualization. GraphMaps reveals the structural properties of the graph and enables users to explore the graph in a natural way by using the standard zoom and pan operations. The available implementation of GraphMaps faces many challenges such as the number of zoom levels may be large, nodes may be unevenly distributed to different levels, shared edges may create ambiguity due to the selection of multiple nodes. In this paper, we develop an algorithmic framework to construct GraphMaps from any given mesh (generated from a 2D point set), and for any given number of zoom levels. We demonstrate our approach introducing competition mesh, which is simple to construct, has a low dilation and high angular resolution. We present an algorithm for assigning nodes to zoom levels that minimizes the change in the number of nodes on visible on the screen while the user zooms in and out between the levels. We think that keeping this change small facilitates smooth browsing of the graph. We also propose new node selection techniques to cope with some of the challenges of the GraphMaps approach.

1 INTRODUCTION

Traditional data visualization systems render all the vertices and edges of the graph on a single screen. For large graphs, this approach requires rendering many objects on the screen, which overwhelms the user. A GraphMaps system confronts the challenge of visualizing large graphs by enabling the users to browse the graphs as interactive maps. Like Google or Bing Maps, a GraphMaps system visualizes the high priority features on the top level, and as we zoom in, the low priority entities start to appear in the subsequent levels. To achieve this effect, for a given graph G and a positive integer $k > 0$, GraphMaps creates the graphs G_1, G_2, \dots, G_k , where G_i , $1 \leq i < k$, is an induced subgraph of G_{i+1} , and $G_k = G$.

The graph G_i , where $1 \leq i \leq k$, corresponds to the i th zoom level. Assume that the nodes of G are ranked by their importance. The discussion on what a node importance is and how the ranking is obtained, is out of the scope of the paper, but by default GraphMaps uses Pagerank (Brin and Page, 2012) to obtain such a ranking. Let $V(G_i)$ be the nodes of G_i . We build graphs G_i in such a way that the nodes of G_i are equally or more important than the nodes

of $V(G_{i+1}) \setminus V(G_i)$. At the top view, we render the graph G_1 . As we zoom in and the zoom reaches 2^{i-1} , the rendering switches from G_{i-1} to G_i , exposing less important nodes and their incident edges. To create spatial stability GraphMaps keeps the node positions fixed, and the rendering of edges changes incrementally between G_i and G_{i+1} as described in Section 3.

By browsing a graph with GraphMaps, the user obtains a quick overview of the important elements. Navigation through different zoom levels reveals the structure of the graph. In addition, users can interact with the system. For example, when the user clicks on a node u , the visualization highlights and renders all neighbors of u (even those that do not belong to the current G_i) and the edges that connect u to its neighbors. By using this interaction the user can explore a path by selecting a set of successive nodes on the path, and can answer adjacency questions by selecting the corresponding pair of nodes.

We draw the nodes as points, and edges as polygonal chains. Each maximal straight line segment in the drawing is called a *rail*. The edges may share rails. Every point where a pair of rails meet is either a node or a point which we call a *junction*. Figure 1(a) depicts a traditional node-link diagram of a

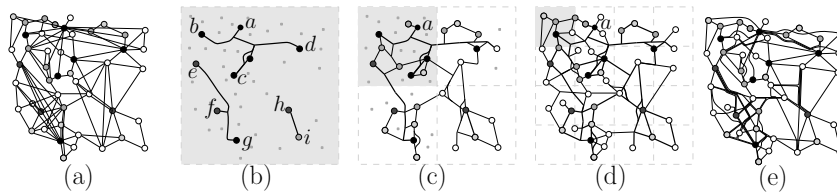


Figure 1: (a) A node-link diagram of a graph G . (b–d) A GraphMaps visualization of G . (e) An example of edge bundling.

graph G . Figures 1(b–c) illustrate a GraphMaps visualization of G on three zoom levels. The gray region at each level corresponds to a viewport in that level. The higher ranked nodes of G have the darker color. The tiny gray dots represent the locations of the nodes that are not visible in the current layer. Figures 2 illustrate the node selection technique and the zoom feature. The rails rendered by thick lines correspond to the shortest paths from the selected nodes a and h to their neighbors.

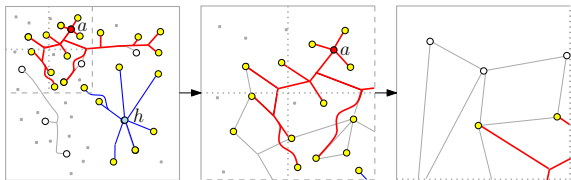


Figure 2: Node selections and zoom in.

In our scheme, where we change the rendering depending on the zoom level, the quality of the visualization depends both on the quality of the drawing on each level, and the differences between the drawings of successive zoom levels. We think that a good drawing of a graph on a single zoom level satisfies the following properties:

- The angular resolution is large
- The *degree* at a node or at a junction is small.
- The amount of *ink*, that is the sum of the lengths of all distinct rails used in the drawing, is small.
- The *edge stretch factor* or *dilation*, that is the ratio of the length of an edge route to the Euclidean distance between its end nodes, is small.

These properties help to follow the edge routes, reduce the visual load, and thus improve the readability of a drawing. Since some of the principles contradict each other, optimizing all of them simultaneously is a difficult task.

Our algorithm, in addition to creating a good drawing of each G_i , attempts to construct these drawings in a way that a switch from G_i to G_{i+1} does not cause a large change on the screen. We try to keep the amount of new appearing details relatively small and also try to keep the edge geometry stable.

1.1 Related Work

A large number of graph visualization tools, e.g., Centrifuge, Cytoscape, Gephi, Graphviz, Biolayout3d, have been developed over the past few decades due to a growing interest in exploring network data. A good visualization requires the careful placement of nodes, e.g., sometimes nodes with similar properties are placed close to each other, whereas the nodes that are dissimilar are placed far away. Force directed approaches, multi-dimensional scaling and stochastic neighbor embedding are some common techniques to generate the node positions (Hu, 2005; Klimentka and Brandes, 2012; van der Maaten and Hinton, 2008). Techniques that try to make the visualization readable by drawing the edges carefully consider various types of edge bundling (Ersoy et al., 2011; Gansner et al., 2011; Lambert et al., 2010; Pupyrev et al., 2011) and edge routing techniques (Dobkin et al., 1997; Holten and van Wijk, 2009; Dwyer and Nachmanson, 2009). Informally, the edge bundling technique groups the edges that are travelling towards a common direction, and routes these edges through some narrow tunnel. Figure 1(e) illustrates an example of edge bundling. Other forms of clutter reduction approaches include node aggregation (Wattenberg, 2006; Dunne and Shneiderman, 2013; Zinsmaier et al., 2012), topology compression (Shi et al., 2013; Brunel et al., 2014), and sampling algorithms (Gao et al., 2014).

This paper focuses on GraphMaps, proposed by Nachmanson et al. (Nachmanson et al., 2015), that reduces clutter by distributing nodes to different zoom levels and routing edges on shared rails. Like the clutter reduction approaches, a primary goal of GraphMaps is to make the visualization more readable and interactive in the higher levels of abstraction. Nachmanson et al. (Nachmanson et al., 2015) use multidimensional scaling to create the node positions. To distribute the nodes into zoom levels, they consider at each level i , an uniform $2^i \times 2^i$ grid, where each grid cell is called a *tile*. The tiles are filled with nodes, the most important nodes first. While filling the levels with nodes, they maintain a node and a rail quota that bound the number of nodes and rails intersecting a tile. Whenever an insertion of a new node creates a tile intersecting more than one fourth of the

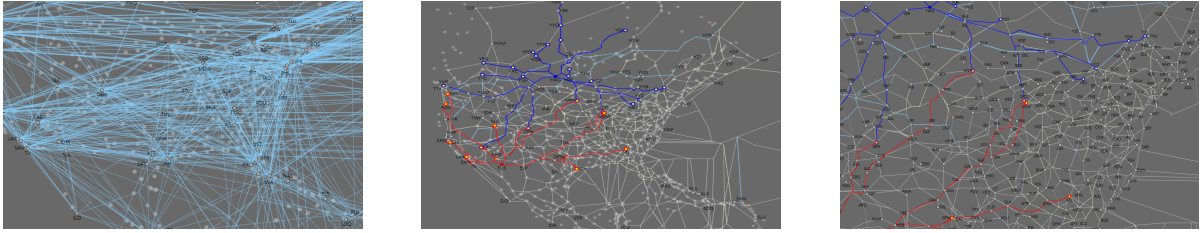


Figure 3: A partial display of a flight network with approximately 3K nodes and 19K edges. (left) Traditional node-link diagram over the airports of North America. (middle) The top-level of a GraphMaps visualization based on our approach, where the airports TUS and YWG are selected. (right) A view after zoom in.

node quota nodes or more than one quarter of rail quota rails, a new zoom level is created to insert the rest of the entities. The visualization of GraphMaps works in such a way that each viewport is covered by four tiles of the current level. This ensures that not more than the node quota nodes and the rail quota rails are rendered per viewport.

GraphMaps visualization also relates to the hierarchical visualization of clustered networks (Schaffer et al., 1996; Balzer and Deussen, 2007). We refer the reader to the survey (Vehlow et al., 2015) for more details on visualizing graphs based on graph partitioning. There exist some systems that render large graphs on multiple layers by using the notion of temporal graphs, e.g., evolving software systems (Collberg et al., 2003; Lambert et al., 2010). A generalization of stochastic neighbor embedding renders nodes on multiple maps (van der Maaten and Hinton, 2012). Gansner et al. (Gansner et al., 2010) proposed a visualization that emphasizes node clusters as geographic regions.

1.2 Contribution

The existing implementation of GraphMaps (Nachmanson et al., 2015) focuses mainly on the quality of the layout at individual zoom level. The construction follows a top-down approach, where the successive levels were obtained by inserting nodes incrementally in a greedy manner.

We propose an algorithm to construct a GraphMaps visualization starting from a complete drawing of the graph $G(= G_k)$ at the bottom level. Specifically, given an arbitrary mesh and the edge routes of G_k on this mesh, our method builds the edge routes for G_{k-1}, \dots, G_2, G_1 , in this order. We introduce a particular type of mesh, called competition mesh, which is of independent interest due to its low edge stretch factor $(2 + \sqrt{2})$, and high angular resolution 45° . We then construct GraphMaps visualizations by applying our algorithm to this mesh. We develop a node assignment algorithm that minimizes

the change in the drawing when switching from G_i to G_{i+1} during zoom in, where $1 \leq i < k$. Moreover, we propose new node selection techniques to cope with some of the challenges of the GraphMaps approach.

We also carried out experiments on some real-life datasets (see Figure 3 and Section 5). Our experiments reveal the usefulness of GraphMaps, even in its basic implementations, for understanding the network information through interactive exploration.

2 TECHNICAL BACKGROUND

We now introduce the mesh that we use for edge routing and analyze its properties. Let P be a set of n distinct points that correspond to the node positions, and let $R(P)$ be the smallest axis aligned rectangle that encloses all the points of P . A *competition mesh* of P is a geometric graph constructed by shooting from each point, four axis-aligned rays at the same constant speed (towards the top, bottom, left and right), where each ray stops as soon as it hits any other ray or $R(P)$. We break the ties arbitrarily, i.e., if two non-parallel rays hit each other simultaneously, then arbitrarily one of these rays stops and the other ray continues. If two rays are collinear and hit each other from the opposite sides, then both rays stop. We denote this graph by $M(P)$, e.g., see Figure 4. The vertices of $M(P)$ are the points of P (*nodes*), and the points where a pair of the rays meet (*junctions*). Two vertices in $M(P)$ are adjacent if and only if the straight line segment connecting them belongs to $M(P)$. A competition mesh can also be viewed as a variation of a motorcycle graph (Eppstein et al., 2008), or a geometric spanner with Steiner points (Bose and Smid, 2013). In the rest of the paper the term ‘vertices’ denotes all the nodes and junctions of $M(P)$.

For any point u , let u_x and u_y be the x and y -coordinates of u , respectively, and let $l_v(u)$ and $l_h(u)$ be the vertical and horizontal straight lines through u , respectively. For any two points p, q in \mathbb{R}^2 , let $dist_E(p, q)$ be the Euclidean distance between p and

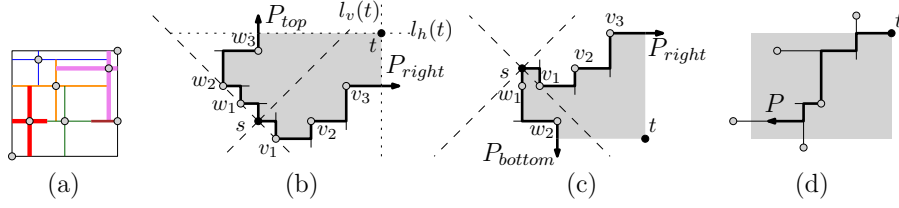


Figure 4: (a) A point set and its corresponding competition mesh. (b–c) Bounding the bottom-left quadrant of t . (d) A monotone path inside the bottom-left quadrant of t .

q . For each point u of the plane we define four *quadrants* formed by the horizontal and vertical lines passing through u . A path v_1, \dots, v_k is *monotone* in direction of vector \mathbf{a} if for each $1 \leq i < k$ the dot product $\mathbf{a} \cdot (v_{i+1} - v_i)$ is not negative. Lemmas 1–2 prove some properties of $M(P)$.

Lemma 1. *Let u be a node in $M(P)$. Then in each quadrant of u there is a path in $M(P)$ that starts at u , ends at some point on $R(P)$, and is monotone in both horizontal and vertical directions.*

Proof. Without loss of generality it suffices to prove the lemma for the first quadrant of u , which consists of the set of points v such that $v_x \geq u_x$ and $v_y \geq u_y$. Suppose for a contradiction that there is no such path in this quadrant. Consider a maximal xy -monotone path Π that starts at u and ends at some node or junction w of $M(P)$. If w is a node, then we extend Π using the right or top ray of w , which is a contradiction. Therefore, w must be a junction in $M(P)$. Without loss of generality assume that the straight line segment ℓ incident to w is horizontal. Since Π is a maximal xy -monotone path, the ray r_ℓ corresponding to ℓ must be stopped by some vertical ray r' generated by some vertex w' . Observe that $w_y > w'_y$, otherwise we can extend Π towards w' . Since r_ℓ is stopped, the ray r' must continue unless there are some other downward ray r'' that hits r' at w . In both cases we can extend Π , either by following r' (if it continues), or following the source of r'' (if r' is stopped by r''), which contradicts to the assumption that Π is maximal. \square

Lemma 2. *For any set P with n points $M(P)$ has $O(n)$ vertices and edges. The graph distance between any two nodes of $M(P)$ is at most $(2 + \sqrt{2})$ times the Euclidean distance.*

Proof. By construction of $M(P)$, whenever a junction is created, one ray stops. Since $|P| = n$ there are at most $4n$ rails, and therefore we cannot have more than $4n$ junctions, that proves that the number of vertices in $M(P)$ is $O(n)$. Since M is a planar graph, the number of edges is also $O(n)$.

We now show that the ratio of the graph distance and the Euclidean distance between any two nodes of

$M(P)$ is at most $(2 + \sqrt{2})$. Let $C_{left}, C_{right}, C_{top}$, and C_{bottom} be the four cones with the apex at $(0,0)$ determined by the lines $y = \pm x$. Let s and t be two nodes in $M(P)$. Without loss of generality assume that s located at $(0,0)$ and t lies on C_{right} . Consider now an x -monotone orthogonal path $P_{right} = (v_0, v_1, v_2, \dots, v_q)$ in the mesh such that v_0 coincides with s , for each $0 < i \leq q$, v_i is a node in $M(P)$ that stops the rightward ray of v_{i-1} , and v_q lies on or to the right of $l_v(t)$, e.g., see Figure 4(b). Suppose that t is either above or below P_{right} . If t is above P_{right} , then consider a y -monotone path $P_{top} = (w_0, w_1, w_2, \dots, w_r)$ such that w_0 coincides with s , for each $0 < i \leq r$, w_i is a node in $M(P)$ that stops the upward ray of v_{i-1} , and w_r lies on or above $l_h(t)$. If t is below P_{right} , then define a path P_{bottom} symmetrically, e.g., see Figure 4(c).

Without loss of generality assume that t is above P_{right} . Observe that the paths P_{top} and P_{right} remain inside the cones C_{top} and C_{right} , respectively, and bound the bottom-left quadrant of t , as shown in the shaded region in Figure 4(b). By Lemma 1, t has a $(-x)(-y)$ -monotone path P that starts at t and reaches the boundary of $R(P)$, e.g., see Figure 4(d). This path P must intersect either P_{top} or P_{right} . Hence we can find a path P' from s to t , where P' starts at s , travels along either P_{top} or P_{right} depending on which one P intersects, and then follows P from the intersection point. We now show that length of P' is at most $(2 + \sqrt{2}) \cdot \text{dist}_E(s, t)$. Since any ray is not shorter than a ray it stops, the sum of the lengths of the vertical segments of P_{right} is at most the sum of the lengths of the horizontal segments. Therefore, the part of P_{right} inside the bottom-left quadrant of t is at most $2t_x$. Similarly, the part of P_{top} inside the bottom-left quadrant of t is at most $2t_y$. Path P is not longer than $t_x + t_y$ (see Figure 4(d)). Therefore, the length of P' is at most $t_x + t_y + 2 \cdot \max\{t_x, t_y\} \leq \sqrt{2} \cdot \text{dist}_E(s, t) + 2 \cdot \max\{t_x, t_y\} \leq (2 + \sqrt{2}) \cdot \text{dist}_E(s, t)$.

In the case when t belongs to P_{right} , the length of path P is zero and the proof easily follows. \square

The following lemma states that a competition mesh can be constructed in $O(n \log n)$ time.

Lemma 3. *For any set P with n points, the competition mesh $M(P)$ can be constructed in $O(n \log n)$ time.*

Proof. Define for each point $w \in P$, a set of eight non-overlapping cones as follows: The central angle of each cone is 45° and the cones are ordered counter clockwise around w . The first cone lies in the first quadrant of w between the lines $y = x + w_x$ and $y = 0$, as shown in Figure 5(a). Guibas and Stolfi (Guibas and Stolfi, 1983) showed that in $O(n \log n)$ time, one can find for every point $w \in P$ the nearest neighbor of w (according to the Manhattan Metric) in each of the eight cones of w . Assume that $\delta_y = \{\min_{\{a,b\} \in P, \text{ where } a_y \neq b_y} |a_y - b_y|\}$, which can be computed in $O(n \log n)$ time by sorting the points according to y -coordinates.

We construct M in four phases. The first phase iterates through the top rays of the each point w and finds the point w' closest to $l(h)_w$ (in Manhattan metric) such that $|w'_x - w_x| \leq |w'_y - w_y|$. Note that if such a w' exists, then one of the horizontal rays r' of w' would reach the point (w_x, w'_y) before the top ray r of w (while all rays are grown in an uniform speed). According to the definition of the competition mesh, we can continue the ray r' and stop growing the ray r . If no such w' exists, then r must hit $R(P)$.

To find the point w' , it suffices to compare the Manhattan distances of the nearest neighbors in the second and third cones of w (breaking ties arbitrarily). Since the nearest neighbors at each cone can be accessed in $O(1)$ time, we can process all the top rays in linear time. Figure 5(b) shows the junctions and nodes created after the first phase, where all the rays that stopped growing are shown in thin lines. The nearest neighbors in the second and third cones of w are a and b , respectively. Since a is closer to $l_h(w)$ than b , the top ray of w does not grow beyond (w_x, a_x) . The second phase processes the bottom rays in a similar fashion, e.g., see Figure 5(c). Both the first and second phase use a ray shooting data structure to check whether the current ray already hits an existing ray. We describe this data structure in the next paragraph while discussing phase three. Let the planar subdivision at the end of phase two be S .

In the third phase, we grow each left ray until it hits any other vertical segment in S , as follows: For each vertical edge ab in S , construct a segment $a'b'$ by shrinking ab by $\delta_y/3$ from both ends. For each node and junction w , construct a segment w_1w_2 such that $w_1 = (w_x, w_y - \delta_y/4)$ and $w_2 = (w_x, w_y + \delta_y/4)$. Let S_v be the constructed segments. Note that the segments in S_v are non-intersecting. Giyora and Kaplan (Giyora and Kaplan, 2009) gave a ray shooting data structure D that can process $O(n)$ non-intersecting vertical rays in $O(n \log n)$ time, and given a query point

q , D can find in $O(\log n)$ time the segment (if any) in S_v immediately to the left of q . Furthermore, D supports insertion and deletion in $O(\log n)$ time. For each point $q \in P$ in the increasing order of x -coordinates, we shoot a leftward ray r from q , and find the first segment ab hit by the ray. Assume that $a_y < b_y$ and r hits ab at point x . We update the subdivision S accordingly, then delete segment ab from D , and insert segment xb in D . Note that these updates keep all the segments in D non-intersecting. Since there are $O(n)$ left rays, processing all these rays takes $O(n \log n)$ time. Figure 5(d) illustrates the third phase.

The fourth phase processes the right rays in a similar fashion, e.g., see Figure 5(e). Since the preprocessing time of the data structures we use is $O(n \log n)$, and since each phase runs in $O(n \log n)$ time, the construction of the computation mesh takes $O(n \log n)$ time in total. \square

3 GRAPHMAPS SYSTEM

Our technique for calculating the graphs G_1, \dots, G_k (equivalently, node level assignment) is described in Section 4. For now, let us assume that the sequence of graphs is ready. We now show how to route edges on graphs G_i .

The computation of edges starts from the bottom. Namely we build a competition mesh M for graph $G(= G_k)$. We route each edge $(u, v) \in G$ as a shortest path P_{uv} in M . Let us denote by M' the mesh we obtain after applying these modifications to M . Next we modify M' to make the routes more visually appealing. We perform local modifications and try to minimize the total ink of the routes, which is the sum of lengths of edges of M' used in the routes (Gansner and Koren, 2006), and remove thin faces. During the modifications we keep the angular resolution greater or equal than some $\alpha > 0$, and the minimum distance between non-incident vertices and edges of M' greater or equal than some $\beta > 0$. The local modifications are described below.

Face refinement: For each face f of M' that does not contain a node of G in its boundary, we compute the width of f , which is the smallest Euclidean distance between any two non-adjacent rails of f . If the width of f is smaller than some given threshold, then remove the longest edge of f from M' (breaking ties arbitrarily). Figures 6(a–b) depict such a removal, where the thin face is shown in gray. The edge routes using the removed edge are rerouted through the remaining boundary of f' .

Median: Move each junction κ of M' toward the geometric median of its neighbors, i.e., the point that

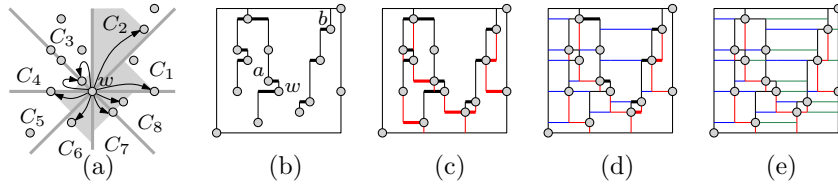


Figure 5: (a) A point set P and the nearest neighbor of w in each of the eight cones around w . (b–e) Construction of the mesh of P , while processing (b) top rays, (c) bottom rays, (d) left rays and (e) right rays.

minimizes the sum of distance to the neighbors, as long as the restriction mentioned above holds. Iterate the move for a certain number of times, or until the change becomes smaller than some given threshold. Figures 6(c–d) illustrate the outcome of this step.

Shortcut: Remove every degree two junction and replace the two edges adjacent to it by the edge short-cutting the removed junction, as long as the restriction mentioned above holds.

In all the above modifications, the routes are updated accordingly. Modifications “Median” and “Shortcut” diminish the ink. The final M' gives the geometry of the bottom-level drawing of G in our version of GraphMaps.

Given a mesh M_i representing the geometry for the drawing of G_i , where $1 < i \leq k$, we construct M_{i-1} from M_i by removing from the latter the nodes $V(G_i) \setminus V(G_{i-1})$, and by removing the edges that are not used by any route $P_{u,v}$, where (u, v) is an edge of G_{i-1} . Some routes $P_{u,v}$ can be straightened in M_{i-1} . We use the simplification algorithm (Douglas and Peucker, 1973) to morph the paths of M_i to paths of M_{i-1} . Figures 7(a–b) illustrate the simplification.

This change in the edge routes geometry diminishes the consistency between the drawings of successive levels. To smoothen the differences while transitioning from zoom level i to $i + 1$ we linearly interpolate between the paths of M_i and M_{i+1} , as demonstrated in Figures 7(b–d).

The idea of path simplification and transition via linear interpolation enables us to construct GraphMaps in a bottom-up approach. In fact, the above strategy can be applied to transform any mesh generated from a set of 2D points to a GraphMaps visualization.

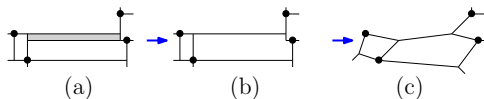


Figure 6: (a–b) Removal of thin faces. (b–c) Moving junctions towards median.

4 COMPUTING NODE LEVELS

Let us consider in more details how the view changes when we zoom by examining Figures 8(a)–(d). On the top-left tile of Figure 8(a), the user’s viewport covers the whole graph, so G_1 is exposed. In Figure 8(d), the user’s viewport contains only the top-left tile of Figure 8(a), and the visualization switches to graph G_2 . Seven new nodes, which were not fully visible in zoom level 1, become fully visible for the current viewport, as represented in light gray. If all of a sudden, a large number of new nodes become fully visible, then it may disrupt user’s mental map. Here we propose an algorithm to keep this change small.

We build the tiles as in (Nachmanson et al., 2015). In the first level we have only one tile coinciding with the graph bounding box. On the i th level, where $i > 1$, the tiles are obtained by splitting each tile in the $(i - 1)$ th level into a uniform 2×2 grid cell. This arrangement of tiles can be considered as a rooted tree T , where the tiles correspond to the nodes of the tree. Specifically, the topmost tile is the root of T , and a node u is a child of another node v if the corresponding tiles t_u and t_v lie in two different but adjacent levels, and $t_u \subset t_v$. We refer to T as a *tile tree*.

For every node v in T , denote by $S(v)$ the number of fully visible nodes in the tile t_v . For an edge $e = (v, w)$ in T , where v is a parent of w , we denote by δ_e the number of new nodes that become visible while navigating from t_v to t_w , i.e., $\delta_e = |S(w) \setminus S(v)|$. We can control the rate the nodes appear and disappear from the viewport by minimizing $\sum_{e \in E(T)} \delta_e^2$, where $E(T)$ is the set of edges in T . For simplicity we show how to solve the problem in one dimension, where all the points are lying on a horizontal line. It is straightforward to extend the technique in \mathbb{R}^2 .

Problem. BALANCED VISUALIZATION

Input. A set P of n points on a horizontal line, where every point $q \in P$ is assigned a rank $r(q)$. A tile tree T of height ρ ; and a node quota Q , i.e., the number of points allowed to appear in each tile.

Output. Compute a mapping $g : P \rightarrow \{1, 2, \dots, \rho\}$ (if exists) that

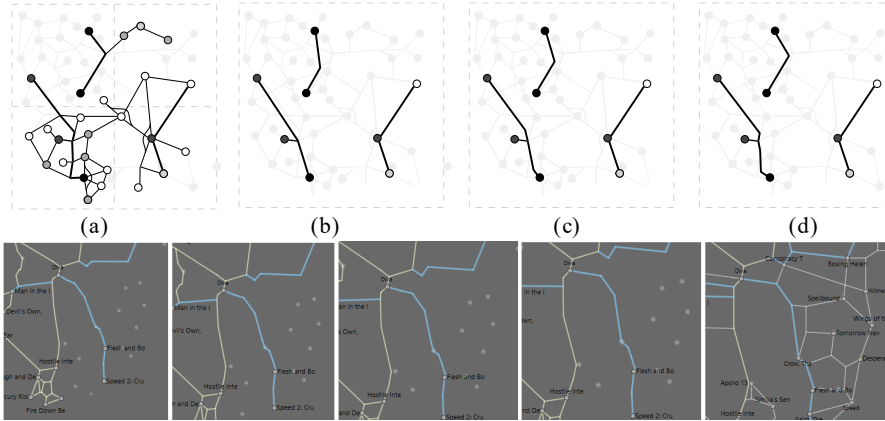


Figure 7: (a) Zoom level 2. (b-d) Transition from level 1 to 2. (bottom) Transition in our GraphMaps system.

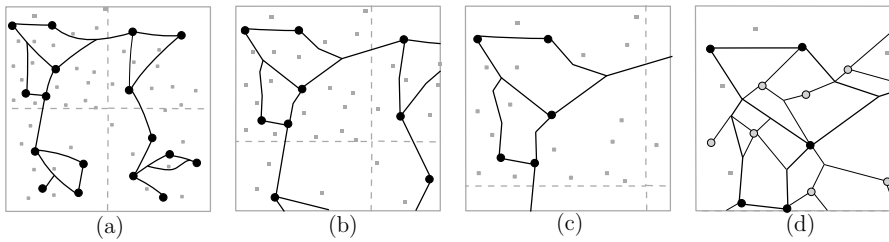


Figure 8: (a) Zoom level 1. (b-c) Transition from level 1 to 2. (d) Zoom level 2.

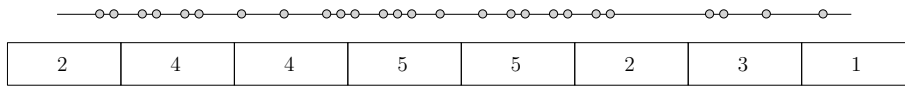
- satisfies the node quota,
- minimizes the objective $F = \sum_{e \in E(T)} \delta_e^2$, and
- for every pair of points $q, q' \in P$ with $r(q) \geq r(q')$, satisfies the inequality $g(q) \leq g(q')$, which we refer to as the *rank condition*.

If the rank of all the points are distinct, then the solution to BALANCED VISUALIZATION is unique, and can be computed in a greedy approach. But the problem becomes non-trivial when many points may have the same rank. In this scenario, we prove that the BALANCED VISUALIZATION problem can be solved in $O(\tau^2 \log^2 \tau) + O(n \log n)$ time, where τ is the number of nodes in T . This is quite fast since the maximum zoom level is a small number, i.e., at most 10, in practice. We reduce the problem to the problem of computing a minimum cost maximum flow problem, where the edge costs can be convex (Orlin, 1993; Orlin and Vaidyanathan, 2013), e.g., quadratic function of the flow passing through the edge. Figure 9(a) depicts a set of points on a line, where the associated tiles are shown using rectangular regions. The numbers in each rectangle is the number of points in the corresponding tile. Figure 9(b) shows a corresponding network G , where the source is denoted by s , and the sinks are denoted by T_1, T_2, \dots, T_8 . The excess at the source and the deficit at the sinks are written in their associated squares. We allow each internal node w (unfilled square) of the tile tree to pass at most Q

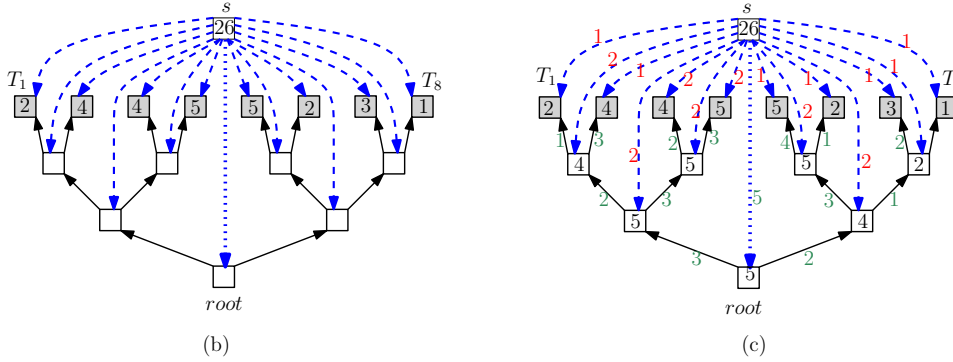
units of flow through it. This can be modeled by replacing w by an edge (u, v) of capacity Q , where all the edges incoming to w are incident to u and the outgoing edges are incident to v . This transformation is not shown in the figure. Set the capacity of all other edges to ∞ .

The production of the source is n units, and the units of flow that each sink can consume is equal to the number of points lying in the corresponding tile. The cost of sending flows along the tree edges (solid black) is zero. The cost of sending flows along the dotted edge connecting the source and the tree root is also zero. The cost of sending x units of flow along the dashed edges is x^2 ; sending x units of flow through a dashed edge corresponds to x new nodes that are becoming visible when we zoom in at the tile of the edge target. Figure 9(c) illustrates a solution to the minimum cost maximum flow problem, where the flows are interpreted as follows:

- The number in a square denotes the number of points that would be visible in the associated tile.
- The edges (s, w) , where w is not the root, are labeled by numbers. Each such number corresponds to the new nodes that will appear while zooming in from the tile associated to $parent(w)$ to the tile associated to w . Thus the cost of this network flow is the sum of the squares of these numbers, i.e., 35.
- Each edge of (u, v) of T is labeled by the number

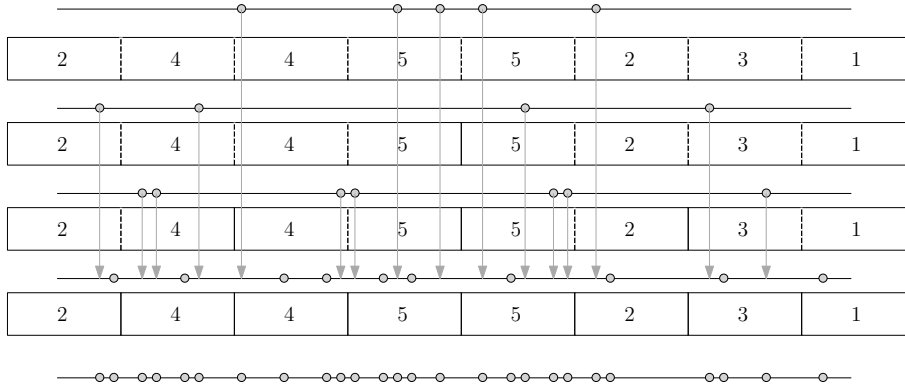


(a)



(b)

(c)



(d)

Figure 9: (a) A set of points on a line and the associated tiles are shown using rectangular regions. (b) A corresponding network G . (c) A solution to the minimum cost maximum flow problem. (d) A solution to the BALANCED VISUALIZATION problem that corresponds to the network flow.

of nodes that are fully visible both u and in v .

- (D) Any one unit source-to-sink flow corresponds to a point of P , where the flow path $source, u_1, u_2, \dots, u_k (= sink)$ denotes that the point appeared in all the tiles associated to u_1, \dots, u_k .

Lemma 4. *A minimum cost maximum flow in G minimizes the objective function F of the BALANCED VISUALIZATION problem.*

Proof. If the amount of flow consumed at sink is smaller than n , then we can find a cut in G with total capacity less than n . Thus even if we saturate the corresponding tiles with points from P , we will not be able to visualize all the points without violating the node quota. Therefore, we can visualize all the points if and only if the flow is maximum and the total consumption is n . Therefore, the only concern is whether the solution with cost λ obtained from flow-network

model minimizes the sum of the squared node differences between every parent and child tiles. Suppose for a contradiction that there exists another solution of BALANCED VISUALIZATION with cost $\lambda' < \lambda$. In this scenario we can label the edges of the network according to the interpretation used in (A)–(D) to obtain a maximum flow in G with cost λ' . Therefore, the minimum cost computed via the flow-network model cannot be λ , a contradiction. \square

Given a solution to the network flow, we can construct a corresponding solution to the BALANCED VISUALIZATION problem as described below.

- For each point w , set $g(w) = \infty$.
- For each zoom level z from ρ to 1, process the tiles of zoom level z as follows. Let W be a tile in zoom level z . Find the amount of flow x incoming to W from s in G . Note that this amount x corresponds to the difference in the number of points between

W and $parent(W)$. Therefore, we find a set L of x lowest priority points in W with zoom level equal to ∞ , then for each $w \in L$, we set $g(w) = z$. Figure 9(d) illustrates a solution to the BALANCED VISUALIZATION problem that corresponds to the network flow of Figure 9(c).

If the resulting mapping does not satisfy the rank condition, then the instance of BALANCED VISUALIZATION does not have any affirmative solution. The best known running time for solving a convex cost network flow problem on a network of size $O(\tau)$ is $O(\tau^2 \log^2 \tau)$ (Orlin, 1993; Orlin and Vaidyanathan, 2013). Besides, it is straightforward to compute the corresponding node assignments in $O(n \log n)$ time augmenting the merge sort technique with basic data structures. Hence we obtain the following theorem.

Theorem 1. *Given a set of n points in \mathbb{R} , a tile tree of τ nodes, and a quota Q , one can find a balanced visualization (if exists) in $O(\tau^2 \log^2 \tau) + O(n \log n)$ time.*

While implementing GraphMaps, we need to choose a node quota Q depending on the given total number of zoom levels p . Using a binary search on the number of nodes, in $O(\log n)$ iterations, one can find a minimal node quota that allow visualizing all the points of P satisfying the rank condition.

5 EXPERIMENTS

The GraphMaps system proposed previously (Nachmanson et al., 2015) uses ¹ to obtain the graph for routing edges on a level. Our approach does not depend on Triangle, but uses Competition Mesh. This has several advantages. For example, Competition Mesh usually produces less edges than Triangle. As a result the edge routing runs much faster. With the same initial layout for the nodes, the GraphMaps system based on our approach sped up the initial processing significantly, up to 8 times on some graphs. The graph with 38395 nodes and 85763 edges was processed in the new system within 1 hour and 45 minutes, where the previous GraphMaps system took 6 hours (Nachmanson et al., 2015). Besides, Competition Mesh is more robust than Triangle. We did not experience failures, which were reported on Triangle (Nachmanson et al., 2015).

The previous GraphMaps (Nachmanson et al., 2015) supports node selection, which is initiated by the user clicks. Selection of a node highlights the paths to its neighbors in red. This may create ambiguity. For example, Figure 10(top-left) shows a

¹<https://www.cs.cmu.edu/~quake/triangle.html>



Figure 10: Node selection in previous GraphMaps (Nachmanson et al., 2015).

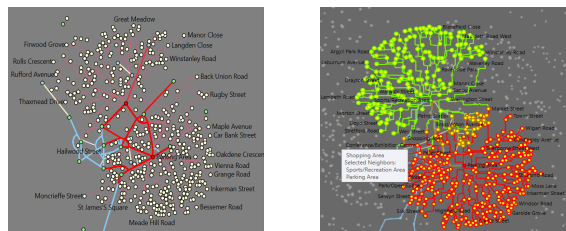


Figure 11: Selection of multiple nodes: (a) previous GraphMaps (Nachmanson et al., 2015), and (b) our approach.

graph of Burglary events (April 2015) in Manchester, UK, where two events are adjacent if they are located within 1km of each other. Selection of the node ‘Burnaby Street’ highlights a rail very close to the node ‘Shopping area’, which gives a false impression that these nodes are adjacent. After zooming in one can see that there is a detour that carries the highlighted path away from ‘Shopping area’, e.g., see Figure 10(top-right). This also give a wrong impression of the node degree. Besides, since the edges may share rails, selection of multiple nodes may obscure the adjacency relationship, e.g., see Figure 11(left).

We introduce new visualizations that allow the user to better understand the node neighborhood. Clicking on a node toggles its status from selected to not selected. When a node is selected, its neighbors are highlighted in yellow color, and the edges connecting the clicked node with the neighbors are highlighted with some unique color. If the mouse pointer hovers over a node highlighted by yellow color, then a tooltip appears with the list of the node neighbors, e.g., see Figure 11(right). When a selected node is unselected, then every edge adjacent to it is rendered in the default color, and the highlighting is removed from each neighbor, unless it is a neighbor of another selected node. These visualization measures help to resolve some ambiguities caused by edge bundling. Note that our approach does not create any detour, and thus avoids the circular artifacts (rails) around the nodes. Exploring the node adjacencies and degree becomes comparatively easy, and less number of rails aids faster level transition.

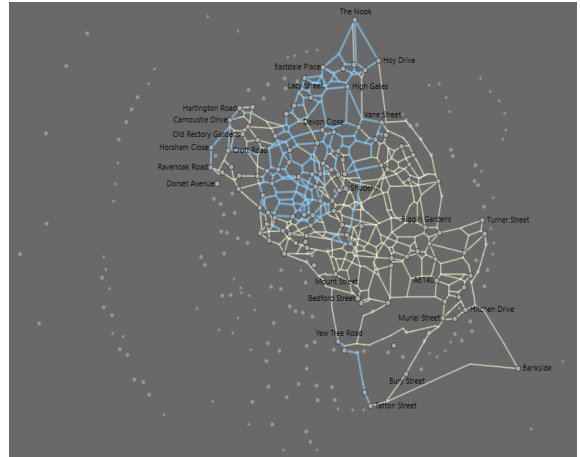
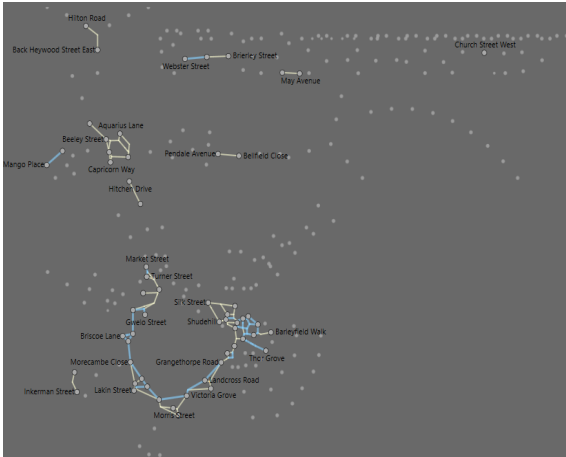


Figure 13: A visualization of drugs-crime event in Manchester, UK, with approximately (left) 0.5K edges, and (right) 8K edges. The rails in light blue and white illustrate the first and second zoom levels, respectively.

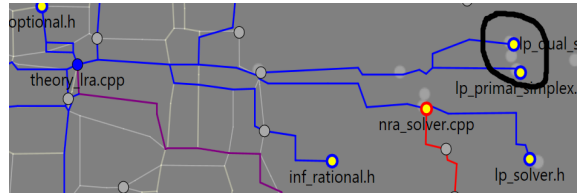
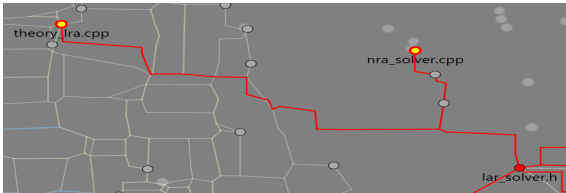


Figure 14: Highlighting the neighborhood in a unique color helps to understand relations.

stretch factor of the competition mesh. It would also be interesting to find bounded degree spanners (possibly with Steiner points) that are monotone and have low stretch factor. We refer the reader to (Bose and Smid, 2013; Dehkordi et al., 2015; Felsner et al., 2016) for more details on such geometric mesh and spanners. We leave it as a future work to examine how the quality of a GraphMaps system may vary depending on the choice of geometric mesh.

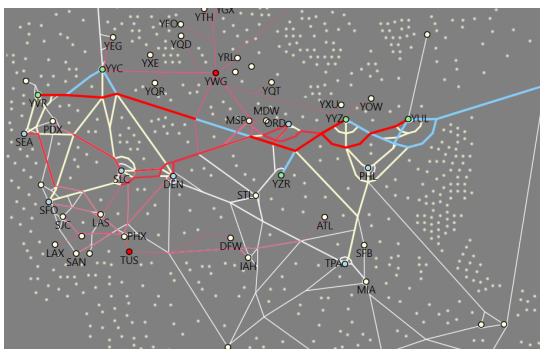


Figure 15: A visualization of the flight network dataset (<https://openflights.org/data.html>) using previous GraphMaps (Nachmanson et al., 2015).

The previous GraphMaps (Nachmanson et al., 2015) uses an incremental mesh generation, which does not require path simplification. Since the con-

struction of the upper levels does not take the lower level nodes into account, the top-level view is usually sparse, e.g., see Figure 15. Our approach is powerful in the sense that any mesh can be transformed into a GraphMaps visualization. But the upper levels are the simplification of the bottom level mesh, and thus the quality of the top-level depends on both the bottom level mesh and the simplification process. It will be interesting to further explore the pros and cons of both approaches. We believe that our results will inspire further research to enhance the appeal and usability of GraphMaps visualizations.

ACKNOWLEDGEMENTS

This work was initiated when the first author was a summer intern at Microsoft Research, Redmond, USA. His subsequent work was partially supported by NSERC.

REFERENCES

Balzer, M. and Deussen, O. (2007). Level-of-detail visualization of clustered graph layouts. In *Asia-Pacific Symp. on Visualization (APVIS)*, pages 133–140. IEEE Computer Society.

- Bose, P. and Smid, M. H. M. (2013). On plane geometric spanners: A survey and open problems. *Computational Geometry*, 46(7):818–830.
- Brin, S. and Page, L. (2012). Reprint of: The anatomy of a large-scale hypertextual web search engine. *Computer Networks*, 56(18):3825–3833.
- Brunel, E., Gemsa, A., Krug, M., Rutter, I., and Wagner, D. (2014). Generalizing geometric graphs. *J. Graph Algorithms Appl.*, 18(1):35–76.
- Collberg, C. S., Kobourov, S. G., Nagra, J., Pitts, J., and Wampler, K. (2003). A system for graph-based visualization of the evolution of software. In *ACM Symp. on Software Visualization (SOFTVIS)*, pages 77–86. ACM.
- Dehkordi, H. R., Frati, F., and Gudmundsson, J. (2015). Increasing-chord graphs on point sets. *J. Graph Algorithms Appl.*, 19(2):761–778.
- Dobkin, D. P., Gansner, E. R., Koutsofios, E., and North, S. C. (1997). Implementing a general-purpose edge router. In *Graph Drawing (GD)*, volume 1353 of *LNCS*, pages 262–271. Springer.
- Douglas, D. and Peucker, T. (1973). Algorithms for the reduction of the number of points required to represent a digitized line or its caricature. *The Canadian Cartographer*, 10(2):112–122.
- Dunne, C. and Shneiderman, B. (2013). Motif simplification: improving network visualization readability with fan, connector, and clique glyphs. In *ACM SIGCHI Conference on Human Factors in Computing Systems (CHI)*, pages 3247–3256. ACM.
- Dwyer, T. and Nachmanson, L. (2009). Fast edge-routing for large graphs. In *Graph Drawing (GD)*, volume 5849 of *LNCS*, pages 147–158. Springer.
- Eppstein, D., Goodrich, M. T., Kim, E., and Tamstorf, R. (2008). Motorcycle graphs: Canonical quad mesh partitioning. *Comput. Graph. Forum*, 27(5):1477–1486.
- Ersoy, O., Hurter, C., Paulovich, F. V., Cantareiro, G., and Telea, A. (2011). Skeleton-based edge bundling for graph visualization. *IEEE Trans. Vis. Comput. Graph.*, 17(12):2364–2373.
- Felsner, S., Igamberdiev, A., Kindermann, P., Klemz, B., Mchedlidze, T., and Scheucher, M. (2016). Strongly monotone drawings of planar graphs. In *Symposium on Computational Geometry*, volume 51 of *LIPIcs*, pages 37:1–37:15.
- Gansner, E. R., Hu, Y., and Kobourov, S. G. (2010). Gmap: Visualizing graphs and clusters as maps. In *IEEE Pacific Visualization Symp. (PacificVis)*, pages 201–208.
- Gansner, E. R., Hu, Y., North, S. C., and Scheidegger, C. E. (2011). Multilevel agglomerative edge bundling for visualizing large graphs. In *IEEE Pacific Visualization Symp. (PacificVis)*, pages 187–194.
- Gansner, E. R. and Koren, Y. (2006). Improved circular layouts. In *Graph Drawing*, pages 386–398. Springer.
- Gao, R., Hu, P., and Lau, W. C. (2014). Graph property preservation under community-based sampling. In *Proceedings of the IEEE Global Communications Conference (GLOBECOM)*, pages 1–7.
- Giyora, Y. and Kaplan, H. (2009). Optimal dynamic vertical ray shooting in rectilinear planar subdivisions. *ACM Transactions on Algorithms*, 5(3).
- Guibas, L. J. and Stolfi, J. (1983). On computing all north-east nearest neighbors in the l_1 metric. *Information Processing Letters*, 17(4):219–223.
- Holtén, D. and van Wijk, J. J. (2009). Force-directed edge bundling for graph visualization. *Comput. Graph. Forum*, 28(3):983–990.
- Hu, Y. (2005). Efficient and high quality force-directed graph drawing. *The Mathematica Journal*, 10:37–71.
- Klimenta, M. and Brandes, U. (2012). Graph drawing by classical multidimensional scaling: New perspectives. In *Graph Drawing (GD)*, volume 7704 of *LNCS*, pages 55–66. Springer.
- Lambert, A., Bourqui, R., and Auber, D. (2010). Winding roads: Routing edges into bundles. *Comput. Graph. Forum*, 29(3):853–862.
- Nachmanson, L., Prutkin, R., Lee, B., Riche, N. H., Holroyd, A. E., and Chen, X. (2015). Graphmaps: Browsing large graphs as interactive maps. In *Graph Drawing & Network Visualization (GD)*, volume 9411 of *LNCS*, pages 3–15. Springer.
- Orlin, J. B. (1993). A faster strongly polynomial minimum cost flow algorithm. *Operations Research*, 41:377–387.
- Orlin, J. B. and Vaidyanathan, B. (2013). Fast algorithms for convex cost flow problems on circles, lines, and trees. *Networks*, 62(4):288–296.
- Pupyrev, S., Nachmanson, L., Bereg, S., and Holroyd, A. E. (2011). Edge routing with ordered bundles. In *Graph Drawing (GD)*, volume 7034 of *LNCS*, pages 136–147. Springer.
- Schaffer, D., Zuo, Z., Greenberg, S., Bartram, L., Dill, J., Dubs, S., and Roseman, M. (1996). Navigating hierarchically clustered networks through fisheye and full-zoom methods. *ACM Trans. Comput.-Hum. Interact.*, 3(2):162–188.
- Shi, L., Liao, Q., Sun, X., Chen, Y., and Lin, C. (2013). Scalable network traffic visualization using compressed graphs. In *IEEE Int. Conference on Big Data*, pages 606–612.
- van der Maaten, L. and Hinton, G. E. (2008). Visualizing data using t-SNE. *Journal of Machine Learning Research*, 9:1–48.
- van der Maaten, L. and Hinton, G. E. (2012). Visualizing non-metric similarities in multiple maps. *Machine Learning*, 87(1):33–55.
- Vehlow, C., Beck, F., and Weiskopf, D. (2015). The State of the Art in Visualizing Group Structures in Graphs. In Borgo, R., Ganovelli, F., and Viola, I., editors, *Eurographics Conference on Visualization (EuroVis) - STARs*. The Eurographics Association.
- Wattenberg, M. (2006). Visual exploration of multivariate graphs. In *Proc. of the Conference on Human Factors in Computing Systems (CHI)*, pages 811–819. ACM.
- Zinsmaier, M., Brandes, U., Deussen, O., and Strobel, H. (2012). Interactive level-of-detail rendering of large graphs. *IEEE Trans. Vis. Comput. Graph.*, 18(12):2486–2495.